

Peng ZW et al. “Integrin $\alpha\beta6$ critically regulates hepatic progenitor cell function and promotes ductular reaction, fibrosis and tumorigenesis”

SUPPLEMENTARY MATERIALS AND METHODS

Hepatic hydroxyproline, as a measure of collagen content was determined biochemically from two liver pieces from the median and left liver lobe (250-300mg in total, representing at least 10% of total liver volume) as described (1). Based on relative hepatic hydroxyproline (per 100mg of wet liver), total hepatic hydroxyproline was calculated (per liver).

Quantitative Real-Time RT-PCR (qRT-PCR) was performed on a LightCycler 1.5 instrument (Roche, Mannheim, Germany) using TaqMan principle as described previously (1, 2). Validated TaqMan probes and primers (**Suppl Table 1**) were obtained commercially or designed using the Primer Express software (Perkin Elmer, Wellesley, USA).

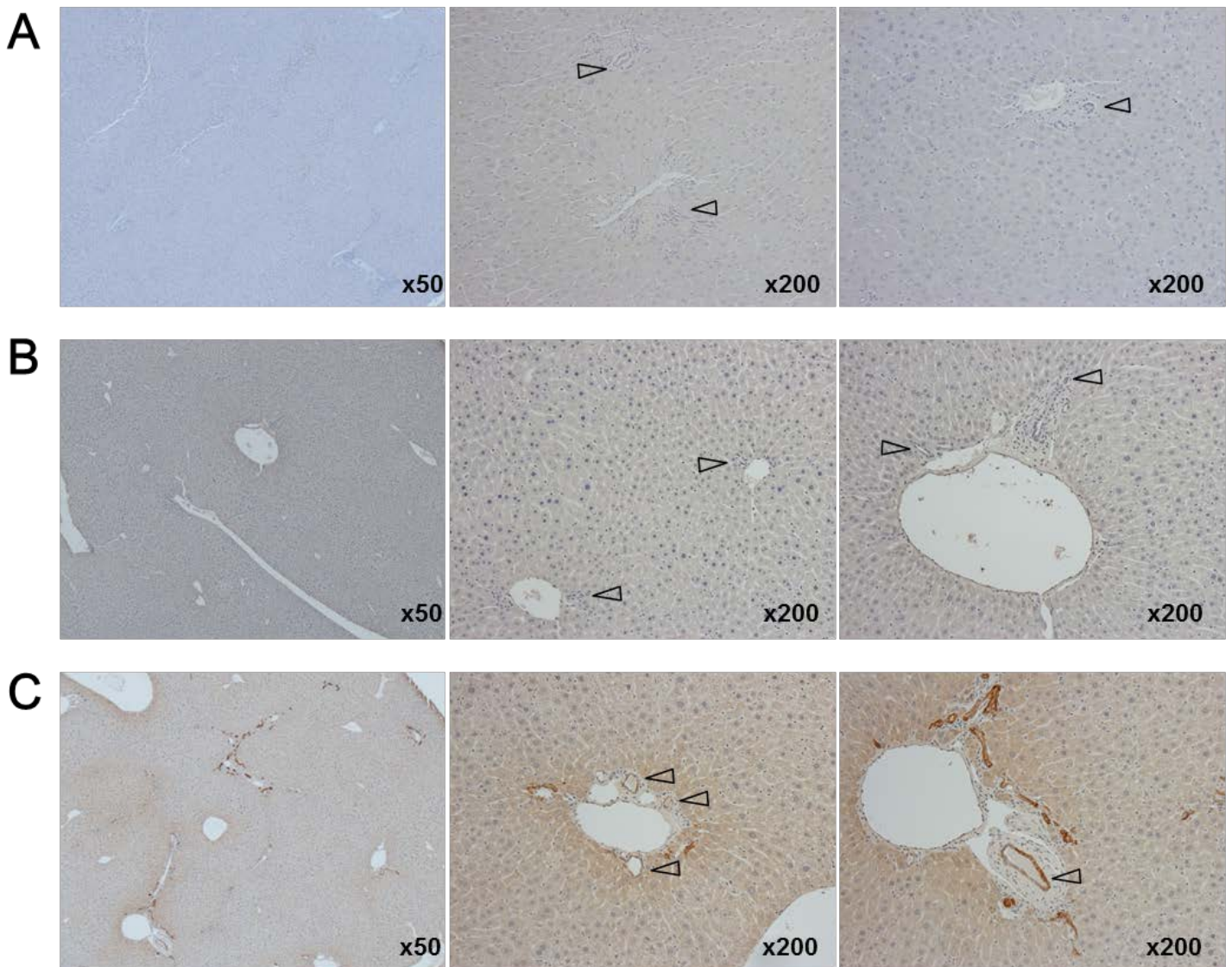
Serum levels of alanine aminotransferase (ALT) were measured on automated Catalyst Dx Chemistry Analyzer (IDEXX Laboratories, Inc., Westbrook, ME) as described (3).

Immunohistochemistry and immunofluorescence for progenitor (oval) cell markers were performed as previously reported(3, 4). Primary antibodies are summarized in Suppl. Table 2. Anti- $\alpha\beta6$ (clone ch2A1, 1/200, Biogen Idec), A6 (1/50, kind gift of Dr. V. Factor, NIH, Bethesda, MD), and anti-pan-cytokeratin (antibodies were used as primary antibodies followed by HRP-conjugated secondary antibodies and DAB reagent. Morphometric analysis was performed by counting positive cells in at least 10 random portal tracts of at least four individual mice/group. Immunofluorescence was performed on acetone-fixed frozen liver sections or cells using primary antibodies against A6 (1/50), PCNA (1/50, Santa Cruz, #sc-7907), $\alpha\beta6$ (clone ch2A1, 1/50, Biogen Idec), TROP2(1/50, AF1122, R&D Systems), pan-cytokeratin (1/50, Z0622, Dako, Glostrup, Denmark), Ki-67(1/200, TEC-3, Dako), K19 (1/200, TROMA-III, Developmental Studies Hybridoma Bank, University of Iowa), followed by secondary fluorophore-conjugated antibodies. DAPI was used as a nuclear counterstain. Images were captured using Zeiss Axioimager M1 (Carl Zeiss, Oberkochen, Germany).

Western blotting for α -SMA was performed and analyzed via band densitometry and normalized to β -actin as a loading control as described(5).

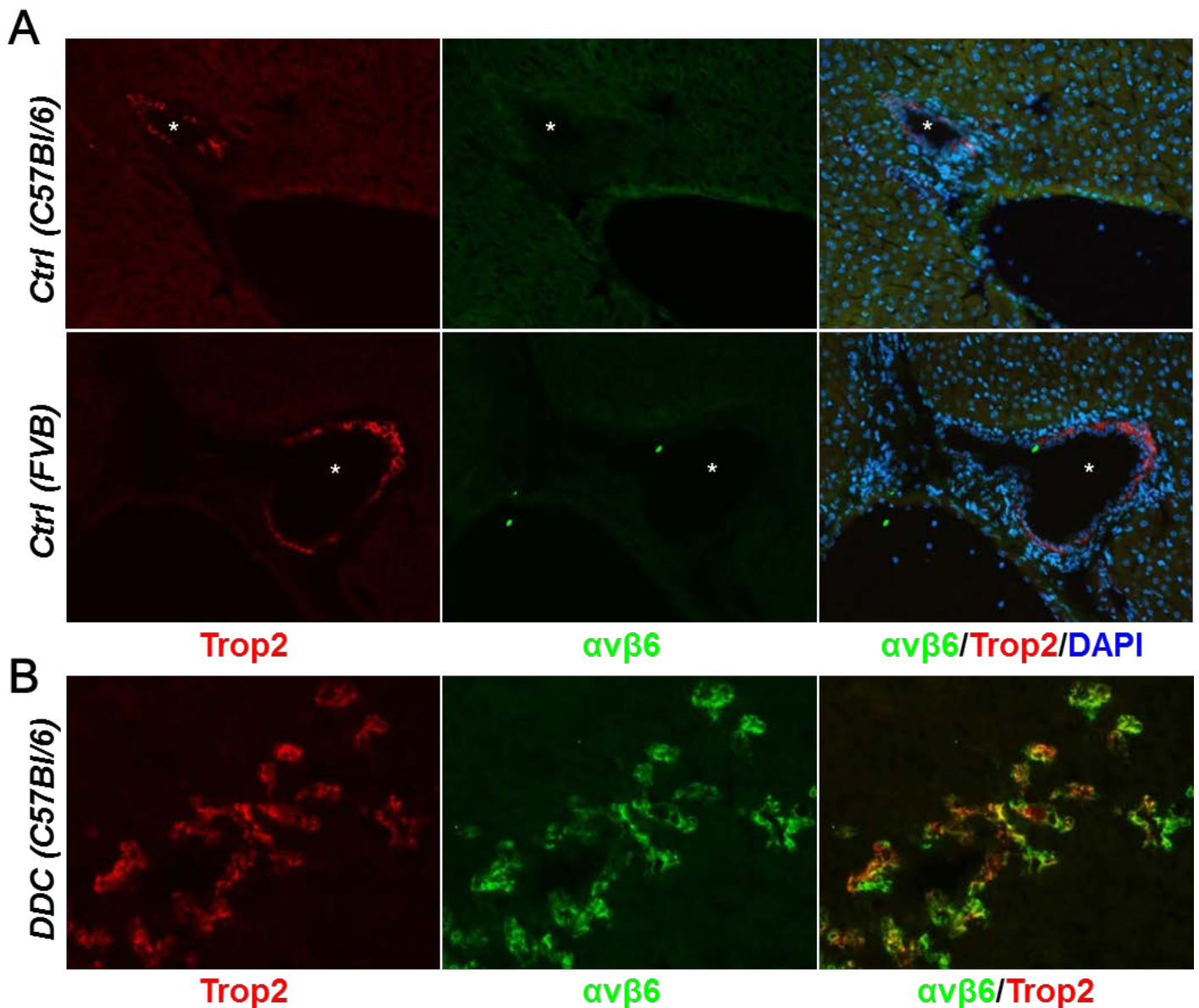
SUPPLEMENTARY RESULTS

Expression pattern of $\alpha\beta6$ integrin in small ductular proliferations constituting ductular reaction and mature cholangiocytes lining larger intrahepatic bile ducts was investigated using immunohistochemistry in normal human and murine livers. No $\alpha\beta6$ expression was detected in either human or murine normal liver (Suppl. Figure 1A and B, respectively). Normal cholangiocytes lining small or large intrahepatic bile ducts, as well as cells in the canals of Hering, were negative for $\alpha\beta6$ (Suppl. Figure 1A and B). In contrast, in fibrotic livers of *Mdr2*^{-/-} mice, intrahepatic bile ducts within fibrotic lesions demonstrated various degrees of $\alpha\beta6$ expression, from strong immune-positivity in some large injured bile ducts to weak or absent expression in smaller and less scarred bile ducts (Suppl. Fig. 1C and Fig. 1A of main manuscript).



Supplementary Figure 1. Integrin $\alpha\beta6$ expression pattern in normal and diseased liver. Immunohistochemistry for $\alpha\beta6$ integrin in normal human liver (A), healthy murine liver (B, wildtype, FVB background) and fibrotic murine liver (C, *Mdr2*^{-/-}, FVB background). Representative images at low (x50, left panel) and high (x200, middle and right panels) shown. Arrows indicate bile ducts.

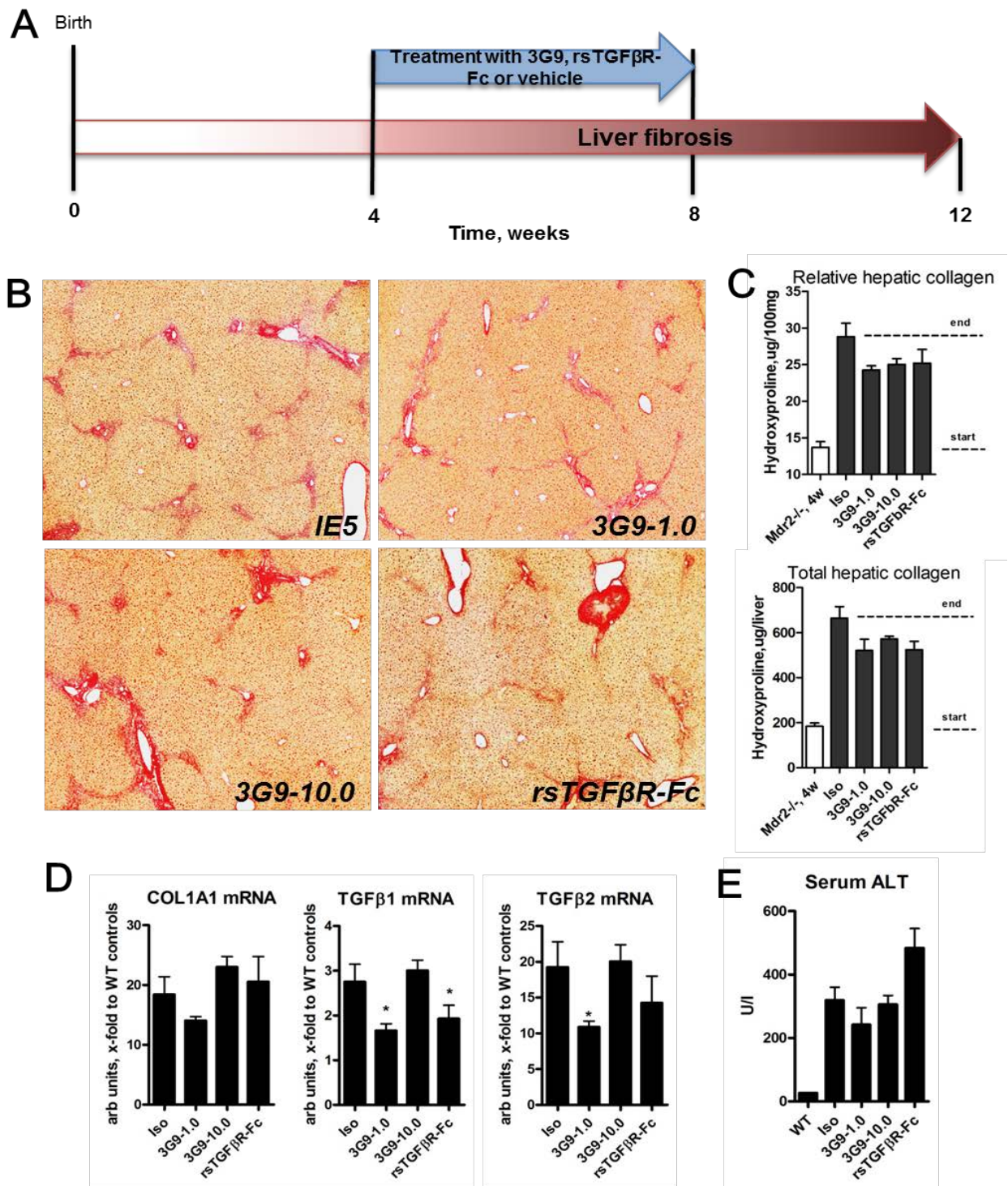
Lack of $\alpha\beta6$ expression on mature normal cholangiocytes was further confirmed using immunofluorescence for $\alpha\beta6$ and progenitor-specific marker Trop2. As expected, small bile ducts in livers of healthy C57Bl/6 and FVB mice were uniformly negative for both $\alpha\beta6$ and Trop2 (not shown). Surprisingly, a few large intrahepatic bile ducts were negative for $\alpha\beta6$ but demonstrated weak Trop2 expression (Suppl. Fig. 2A, exposure time twice as much as in DDC-fed mice images below). In contrast, proliferating cells comprising ductular reaction in chronically injured liver due to DDC feeding demonstrated robust Trop2 and $\alpha\beta6$ expression with almost complete overlap (Suppl. Fig. 2B)



Supplementary Figure 2. Double-immunofluorescence for integrin $\alpha\beta6$ and hepatic progenitor marker Trop2 in normal and diseased murine liver. Immunofluorescence for $\alpha\beta6$ integrin (green) and Trop2 (red) in healthy murine liver (A, wildtype, FVB and C57Bl/6 background) and fibrotic murine liver (B, DDC-fed, C57Bl/6 background). Representative images at x200 magnification shown. Asterisks indicate large intrahepatic bile ducts.

Early treatment with $\alpha\beta6$ -blocking antibody (3G9 mAB) fails to achieve significant antifibrotic effect in *Mdr2*^{-/-} model of chronic biliary injury

To test whether $\alpha\beta6$ inhibition can prevent early-stage biliary fibrosis, we treated 4-week-old *Mdr2*^{-/-} mice (with incipient fibrosis) with anti- $\alpha\beta6$ antibody 3G9 (1 and 10mg/kg weekly i/p) for 4 weeks (early treatment protocol). At the end of treatment, 8-week-old *Mdr2*^{-/-} mice that received isotype control antibody developed significant interstitial fibrosis with occasional bridging septae and significant increases in hepatic collagen levels (Suppl. Fig. 3B,C). Although mice treated with both doses of 3G9 mAB and systemic TGF β inhibition (rsTGF β RII-Fc) showed signs of histological improvement (less ductular proliferation and bridging fibrosis, Suppl. Fig. 3B), hepatic collagen deposition showed a trend to lower values and failed to reach statistical significance (Suppl. Fig. 3). Analysis of fibrosis-related gene expression also did not reveal consistent changes due to $\alpha\beta6$ /TGF β inhibition: procollagen 1 (COL1A1) mRNA did not change, while TGF β 1 decreased by 30-40% in low 3G9 dose and rsTGF β RII-Fc-treated groups, and TGF β 2 was 40% lower only in the low dose 3G9 group (Suppl. Fig. 3D). Serum ALT levels had a trend to higher values in rsTGF β RII-Fc-treated mice, but were not significantly affected by any of the treatments (Suppl. Fig. 3E).

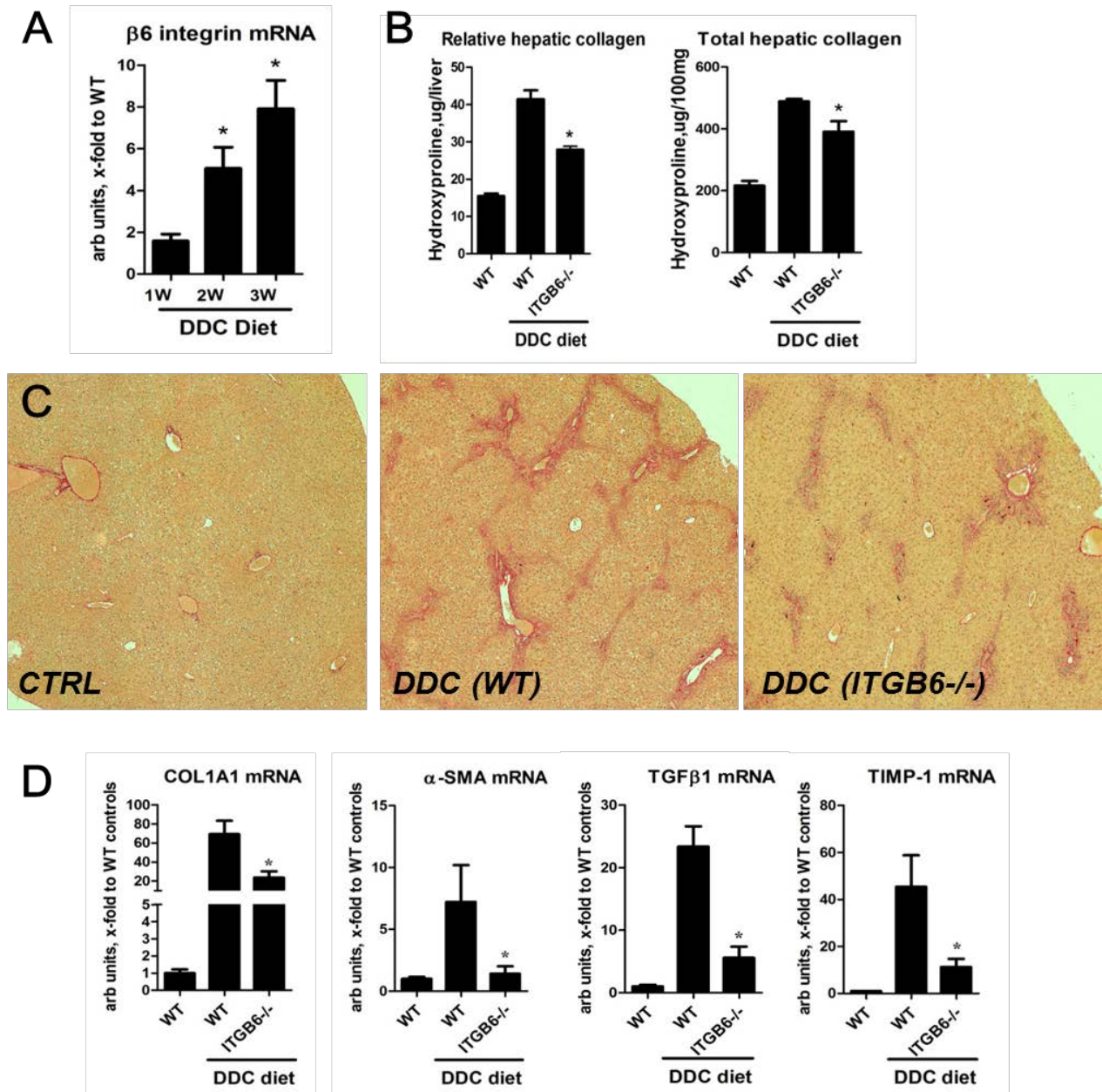


Supplementary Figure 3. Early treatment using function-blocking 3G9 antibody in *Mdr2*^{-/-} mice.

A. Scheme of experimental design. Integrin $\alpha\beta6$ -blocking antibody 3G9 mAb (1 and 10 mg/kg), 1E5 isotype control antibody (10 mg/kg) and rsTGF β RII-Fc protein (5 mg/kg) were administered four times (i.p. once a week) in *Mdr2*^{-/-} mice with incipient biliary fibrosis starting at 4 weeks of age. **B.** Representative low-magnification images of connective tissue (Sirius Red) staining in *Mdr2*^{-/-} mice (original magnification, x50). **C.** Relative (per 100mg of liver) and total (per whole liver) hepatic collagen levels in *Mdr2*^{-/-} mice (biochemically via hydroxyproline). **D.** Hepatic transcript levels of COL1A1 and TGF β 1/2 as determined by real-time RT-PCR in total liver RNA (relative to β 2-microglobulin, expressed as fold to healthy WT controls). **E.** Serum ALT levels in *Mdr2*^{-/-} mice. Data expressed as mean \pm SEM (n=6-8), * p \leq 0.05 compared to isotype control group (ANOVA with Dunett's post-test)

Integrin $\alpha\beta6$ deficiency confers protection from DDC-induced liver fibrosis

Wildtype (WT) C57Bl/6 and *Itgb6*-null mice (C57Bl/6 background) were fed DDC-supplemented diet for 3 weeks to induce oval cell reaction and progressive biliary fibrosis. Integrin beta 6 mRNA was up-regulated progressively up to 8-fold over baseline during 1-3 weeks in DDC model (Suppl. Fig. 4A). After 3 weeks of DDC feeding, WT mice developed sclerosing cholangitis with pronounced ductular reaction and advanced interstitial fibrosis, as expected. Fibrosis was significantly reduced in *Itgb6*^{-/-} mice, with 50% and 30% reductions in relative and total collagen content, respectively, and no bridging fibrosis observed histologically (Suppl. Fig. 4B,C). Fibrosis-related gene expression was suppressed several fold compared to DDC-fed WT mice (Suppl. Fig. 2D). Progenitor responses in *Itgb6*^{-/-} mice, as evaluated by progenitor cell marker A6 and Trop2 staining, were markedly attenuated (Fig. 7 in the main manuscript). Similar results were obtained when staining with pan-cytokeratin, an alternative progenitor cell marker (not shown).



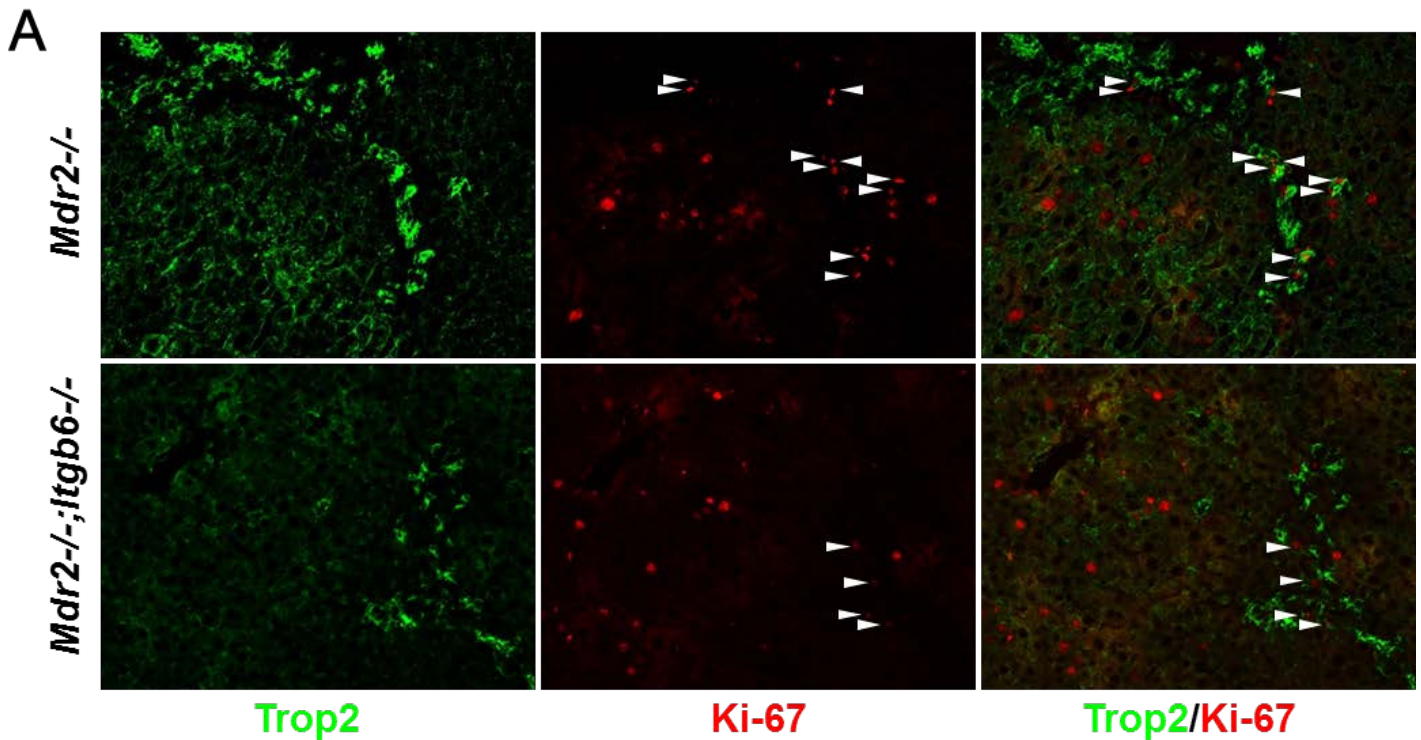
Supplementary Figure 4. Integrin $\alpha\beta6$ deficiency protects from liver fibrosis induced by DDC feeding.

A. Integrin $\beta6$ mRNA expression progressively increased after DDC diet from week 1 to week 3 in wildtype (WT) C57Bl/6 mice. **B.** Relative (per 100mg of liver) and total (per whole liver) hepatic collagen levels in WT and C57Bl/6.*Itgb6*^{-/-} mice after 3 weeks on DDC diet (biochemically via hydroxyproline). **C.** Representative low-magnification images of connective tissue (Sirius Red) staining in WT and *Itgb6*^{-/-} mice with DDC feeding (original magnification, x50). **D.** Hepatic transcript levels of COL1A1, α SMA, TGF β 1 and TIMP-1 as determined by real-time RT-PCR in total liver RNA (relative to β 2-microglobulin, expressed as fold to healthy WT controls). Data expressed as mean \pm SEM (n=6-8), * $p\leq 0.05$ compared to WT on DDC diet (t-test).

Hepatic progenitor cell activation and fibrogenesis is markedly attenuated in the absence of integrin $\alpha\beta6$ in *Mdr2*^{-/-} model of chronic biliary injury

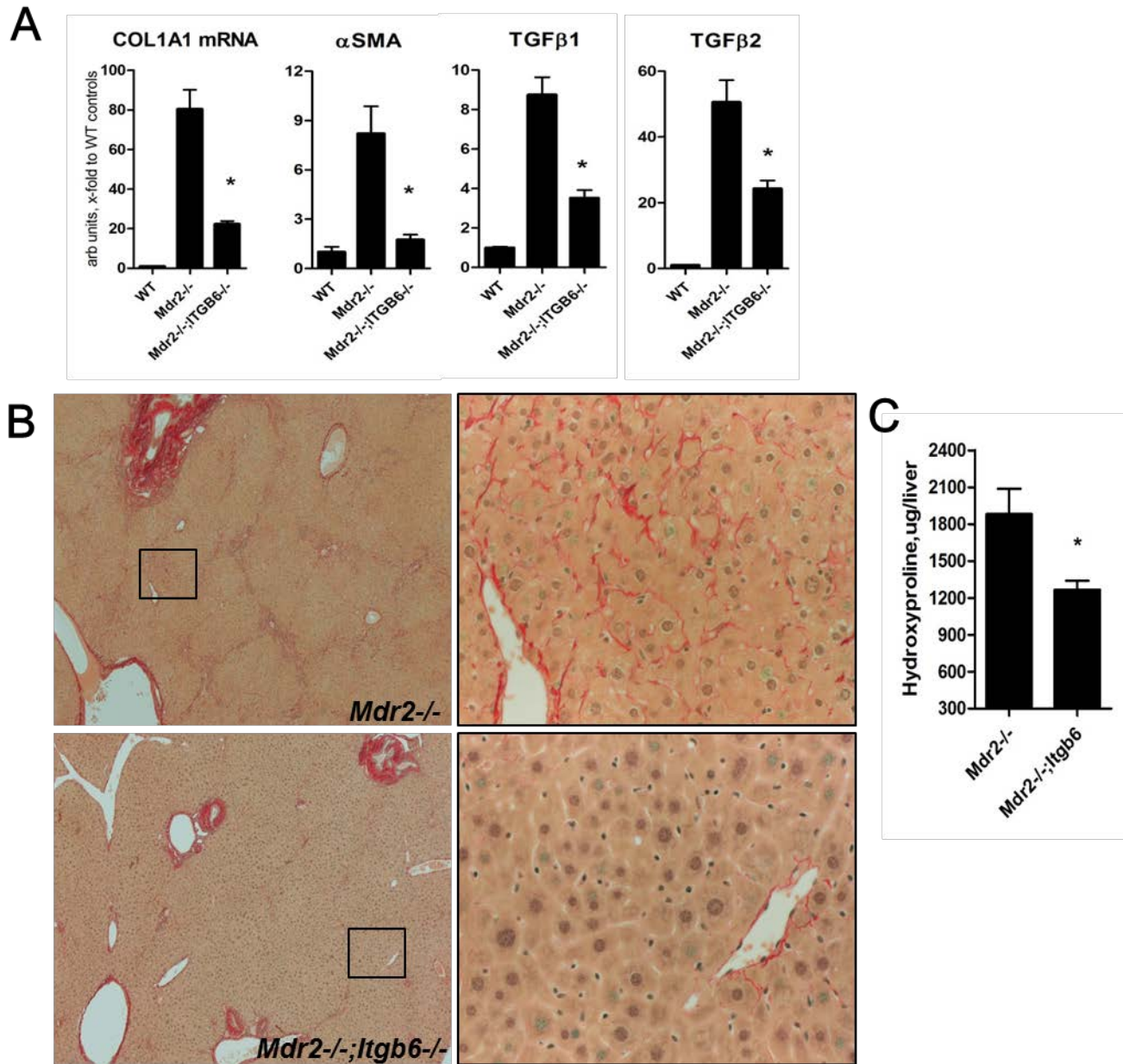
To assess the role of integrin $\alpha\beta6$ in the progenitor response, hepatic fibrosis, and hepatocellular carcinoma, we generated *Mdr2*^{-/-};*Itgb6*^{-/-} double knockouts (as described in M&M) and analyzed them in comparison to integrin $\alpha\beta6$ -sufficient *Mdr2*^{-/-} mice. Analysis of F2 progeny (8 weeks of age) revealed higher hepatic collagen levels in *Mdr2*^{-/-};*Itgb6*^{-/-} mice compared to *Mdr2*^{-/-} littermates (not shown). This was unexpected in the context of significant protection from fibrosis in the DDC model in adult *Itgb6*^{-/-} mice (Suppl. Fig. 4), and the antifibrotic effect of anti- $\alpha\beta6$ antibody treatment at advanced disease stages (Fig. 5 of the main manuscript). Because of the well-documented expression of $\alpha\beta6$ in developing, but not healthy adult liver, we hypothesized that the absence of $\alpha\beta6$ during liver development along with congenital liver disease in *Mdr2*^{-/-} may produce artifacts related to early developmental events rather than fibrogenesis.

To test this, we used a low-dose cholic acid challenge (which aggravates liver injury and fibrosis in *Mdr2*^{-/-} mice (6)) in adult (5week-old) male *Mdr2*^{-/-};*Itgb6*^{-/-} and *Mdr2*^{-/-} mice for 4 weeks, and analyzed the progenitor (oval) cell compartment, liver injury and fibrogenesis. Cholic-acid feeding led to a 3-fold increase in serum ALT levels, which did not differ between *Mdr2*^{-/-};*Itgb6*^{-/-} and *Mdr2*^{-/-} mice (not shown). Histological examination showed that *Mdr2*^{-/-} mice developed severe ductular reaction with expansion of A6⁺ progenitors around portal tracts and along fibrotic septae. However, ductular reaction and progenitor expansion were notably reduced in *Mdr2*^{-/-};*Itgb6*^{-/-} mice, with A6⁺ cell counts reduced by 65% compared to *Mdr2*^{-/-} littermates (See Fig. 6C,D of main manuscript). Double-immunofluorescence for progenitor marker Trop2 and Ki-67 (nuclear cell proliferation antigen) revealed that replication of progenitors appears to be reduced in the absence of integrin $\alpha\beta6$ (Suppl. Fig. 5). The fibrogenic response, as measured by fibrosis-related hepatic mRNA levels, was indeed dramatically attenuated in *Mdr2*^{-/-};*Itgb6*^{-/-} mice (Suppl. Fig. 6A). Accordingly, fibrosis induced by cholic acid challenge (5-9 weeks of age) was significantly inhibited in *Mdr2*^{-/-};*Itgb6*^{-/-}, which deposited less than half of hepatic collagen compared to their *Mdr2*^{-/-} littermates (average increase in hydroxyproline 301.8ug/liver versus 627ug/liver in *Mdr2*^{-/-}, not shown).



Supplementary Figure 5. Integrin $\alpha\beta 6$ deficiency attenuates progenitor cell proliferation in *Mdr2*^{-/-} mice.
A. Double-immunofluorescence for cell proliferation marker Ki-67 (red, arrows) and progenitor marker Trop2 (green) suggest diminished progenitor cell replication (double-positive cells indicated by arrows) in *Mdr2*^{-/-}; *Itgb6*^{-/-} mice (lower panel) compared to *Mdr2*^{-/-} (upper panel). Note similar numbers of proliferating hepatocytes (large Ki-67(+) nuclei within hepatic lobule) between mice of both genotypes. Representative images shown (original magnification, x200).

We kept a parallel groups of *Mdr2*^{-/-} and *Mdr2*^{-/-}; *Itgb6*^{-/-} mice on regular chow for an extended period of time (1 year) for primary liver tumor assessment (see main manuscript), which were also analyzed for fibrotic/cirrhotic outcomes. Liver fibrosis in *Mdr2*^{-/-}; *Itgb6*^{-/-} developed less progressively throughout their life-time compared to *Mdr2*^{-/-}, as evidenced by lack of characteristic cirrhotic changes(5) in aged FVB.*Mdr2*^{-/-} mice such as significant sinusoidal fibrosis (Suppl. Fig. 6B), as well as 33% decrease in hepatic collagen content at 12 months of age (Suppl. Fig. 6C).



Supplementary Figure 6. Fibrogenesis is markedly attenuated in the absence of integrin $\alpha\beta 6$ in double-mutant *Mdr2*^{-/-};*Itgb6*^{-/-} mice.

A. Profibrogenic genes COL1A1, TGF β 1/2 and α SMA expression is strongly diminished in cholic acid-fed *Mdr2*^{-/-};*Itgb6*^{-/-} mice. Hepatic transcript levels of target genes were determined by real-time RT-PCR in total liver RNA (relative to β 2-microglobulin, expressed as fold to healthy WT controls). Data are mean \pm SEM (n=4-5 per bar), **B.** Connective tissue staining in aged mice kept on regular chow (12 months old). Note severe sinusoidal fibrosis in *Mdr2*^{-/-} that is absent in *Mdr2*^{-/-};*Itgb6*^{-/-} mice. Representative Sirius Red images (magnification: left panel, 50x; right panel, 400x). **C.** Hepatic collagen content in 12 months-old *Mdr2*^{-/-} and *Mdr2*^{-/-};*Itgb6*^{-/-} mice on a regular chow. Data are mean \pm SEM (n=12 per bar)*, $p \leq 0.05$ compared to *Itgb6*-sufficient *Mdr2*^{-/-} mice (t-test).

Supplementary Table 1. Primers and probes used in quantitative RT-PCR.

Target gene	5'-Primer	TaqMan probe	3'-Primer
β_2MG	CTGATACATACGCCTGCAGAGTTAA	GACCGTCTACTGGGATCGAGACATGTG	ATGAATCTTCAGAGCATCATGAT
COL1A1	TCCGGCTCCTGCTCCTCTTA	TTCTTGCCATGCGTCAGGAGGG	GTATGCAGCTGACTTCAGGGATGT
TGFβ1	AGAGGTCACCCGCGTGCTAA	ACCGCAACAACGCCATCTATGAGAAAACCA	TCCCGAATGTCTGACGTATTGA
α-SMA	ACAGCCCTCGCACCCA	CAAGATCATTGCCCTCCAGAACGC	GCCACCGATCCAGACAGAGT
TGFβ2	GTCCAGCCGGCGGAA	CGCTTTGGATGCTGCCTACTGCTTTAGAAAT	GCGAAGGCAGCAATTATCCT
Itgb6	GCAGAACGCTCTAAGGCCAA	TGGCAAACGGGAACCAATCCTCTGT	AAAGTGCTGGTGGACCTCG
Fn14	TGCCGCCGAGAGAAAA	CTCTCCACCAGTCTCCTCTATGGGGGTAGTAAA	GCCACACCTGGGCAGC
Albumin	GCTACGGCACAGTGCTTG	-	CAGGATTGCAGACAGATAGTC
TAT	ACGCACAGACGCACGCACTCAC	-	CTTCCGGTCCGCAGCAATGT
K19	GCTGCAGATGACTTCAGAACC	-	CATGGTTCTTTCAGGTAGGC
EpCAM	TTGCAGACTGCGCTTCAAGA	-	TACGATCGGTAATGCCGGTG
CD133	ACCGGAGAGGGATGGTACTT	-	GGCAATCTTCAGAGCCAAGAC
HNF1β	TaqMan assay ID: Mm00447459_m1 (Life Technologies)		
K19	TaqMan assay ID: Mm00492980_m1 (Life Technologies)		
HNF4α	TaqMan assay ID: Mm01247712_m1 (Life Technologies)		
Albumin	TaqMan assay ID: Mm00802090_m1 (Life Technologies)		
Trop2	TaqMan assay ID: Mm00498401_s1 (Life Technologies)		
EpCAM	TaqMan assay ID: Mm000493214_m1 (Life Technologies)		
SOX9	TaqMan assay ID: Mm00448840_m1 (Life Technologies)		
α-Fetoprotein	TaqMan assay ID: Mm00431715_m1 (Life Technologies)		
Foxl1	TaqMan assay ID: Mm00514937_s1 (Life Technologies)		
Lgr5	TaqMan assay ID: Mm00438890_m1 (Life Technologies)		

REFERENCES

1. Popov Y, Sverdlov DY, Sharma AK, Bhaskar KR, Li S, Freitag TL, Lee J, et al. Tissue transglutaminase does not affect fibrotic matrix stability or regression of liver fibrosis in mice. *Gastroenterology* 2011;140:1642-1652.
2. Popov Y, Patsenker E, Stickel F, Zaks J, Bhaskar KR, Niedobitek G, Kolb A, et al. Integrin alphavbeta6 is a marker of the progression of biliary and portal liver fibrosis and a novel target for antifibrotic therapies. *J Hepatol* 2008;48:453-464.
3. Ikenaga N, Liu SB, Sverdlov DY, Yoshida S, Nasser I, Ke Q, Kang PM, et al. A New Mdr2 Mouse Model of Sclerosing Cholangitis with Rapid Fibrosis Progression, Early-Onset Portal Hypertension, and Liver Cancer. *Am J Pathol* 2014.
4. Kuramitsu K, Sverdlov DY, Liu SB, Csizmadia E, Burkly L, Schuppan D, Hanto DW, et al. Failure of fibrotic liver regeneration in mice is linked to a severe fibrogenic response driven by hepatic progenitor cell activation. *Am J Pathol* 2013;183:182-194.
5. Yoshida S, Ikenaga N, Liu SB, Peng ZW, Chung J, Sverdlov DY, Miyamoto M, et al. Extra-hepatic PDGFB, Delivered by Platelets, Promotes Activation of Hepatic Stellate Cells and Biliary Fibrosis in Mice. *Gastroenterology* 2014.
6. Van Nieuwkerk CM, Elferink RP, Groen AK, Ottenhoff R, Tytgat GN, Dingemans KP, Van Den Bergh Weerman MA, et al. Effects of Ursodeoxycholate and cholate feeding on liver disease in FVB mice with a disrupted mdr2 P-glycoprotein gene. *Gastroenterology* 1996;111:165-171.